



## Isolation and characterization of two novel oral bacteriophages with anti-biofilm activity against *Cutibacterium acnes*

Anja Frantar<sup>a,\*</sup>, Katja Seme<sup>b</sup>, Rok Gašperšič<sup>c</sup>, Čedomir Oblak<sup>a</sup>, Katja Šuster<sup>d,e</sup>

<sup>a</sup> Department of Prosthodontics, Faculty of Medicine, University of Ljubljana, Ljubljana 1000, Slovenia

<sup>b</sup> Institute of Microbiology and Immunology, Faculty of Medicine, University of Ljubljana, Ljubljana 1000, Slovenia

<sup>c</sup> Department of Oral Medicine and Periodontology, Faculty of Medicine, University of Ljubljana, Ljubljana 1000, Slovenia

<sup>d</sup> Scientific Research and Educational Department, Valodtra Orthopaedic Hospital, Ankaran 6280, Slovenia

<sup>e</sup> Faculty of Health Sciences, University of Primorska, Koper 6000, Slovenia

### ARTICLE INFO

#### Keywords:

*Cutibacterium acnes*  
Bacteriophage  
Biofilm  
Antibiofilm activity  
Phage therapy  
Genome analysis

### ABSTRACT

Bacteriophage therapy offers a promising solution to combat antibiotic-resistant infections, yet its potential against biofilm-associated pathogens in oral diseases remains underexplored. This study investigates the opportunistic bacterium *Cutibacterium acnes*, an overlooked contributor to dental implant and prosthetic joint infections. Biofilms formed by *C. acnes* are highly resilient and resistant to antibiotics, complicating treatment. Two novel lytic bacteriophages, Ristretto and Corretto, targeting *C. acnes*, were isolated from human saliva, with morphological analysis confirming their classification as siphoviruses. Their genome sequencing revealed no harmful antimicrobial resistance or virulence genes, making them suitable for therapeutic use. Remarkably, phage Corretto demonstrated a broad host range and achieved near-complete eradication of mature biofilms across multiple *C. acnes* strains, outperforming Ristretto in efficacy and strain coverage. The activity of these phages was dosage-dependent and varied across bacterial strains, revealing potential strain-specific resistance mechanisms within biofilms. These findings highlight bacteriophage therapy's potential to disrupt persistent biofilms where antibiotics fail, offering a new approach for treating biofilm-driven infections in dental and medical implantology. This study underscores the need for further research into phage-based strategies to address the growing global challenge of antimicrobial resistance and improve outcomes in biofilm-related diseases.

### 1. Introduction

Implant-associated infections share a defining characteristic: their development depends on microbial biofilms, which are essential to both disease progression and resistance to treatment (Arciola et al., 2018). Medical devices can all be prone to serious and chronic complications if infected, potentially resulting in long-term pain, loss of function, the need for surgical intervention or removal of the device (Herrera et al., 2023; Kennedy et al., 2022; Otto-Lambertz et al., 2017). The most common indwelling devices that are subject to infection are: orthopaedic devices, cardiac devices, dental implants, and intravascular devices, all of which are now widely used in various areas of healthcare (Blomstrom-Lundqvist and Ostrowska, 2021; Weinstein and Darouiche, 2001).

Replacing missing teeth with dental implants is commonly followed

by peri-implantitis, an inflammatory reaction in the mucosa surrounding the implant, triggered by ecological changes and overgrowth of pathogenic species/strains in the microbial biofilm covering oral-cavity-exposed implant surface (Kröger et al., 2018). Peri-implantitis is a site-specific disease that causes bone loss around the implant, which can eventually lead to implant failure (Monje et al., 2019). Unfortunately, there is no universally effective treatment strategy at present. While orthopaedic implants become infected in 1–2 % of primary cases (Ahmed and Haddad, 2019; Alp et al., 2016), infections around dental implants are far more common. Results in studies are highly variable, with an estimated peri-implantitis prevalence ranging around 20 % at the patient level and 10 % at the implant level, making it a relatively frequent complication (Rakic et al., 2018).

From around 1000 bacterial species thriving in oral biofilms (Radaic and Kapila, 2021), only a few are linked to the development of

\* Corresponding author.

E-mail address: [anja.frantar@mf.uni-lj.si](mailto:anja.frantar@mf.uni-lj.si) (A. Frantar).

<https://doi.org/10.1016/j.ijmm.2025.151668>

Received 1 May 2025; Received in revised form 4 August 2025; Accepted 7 August 2025

Available online 7 August 2025

1438-4221/© 2025 The Authors. Published by Elsevier GmbH. This is an open access article under the CC BY license (<http://creativecommons.org/licenses/by/4.0/>).

peri-implantitis. *Cutibacterium acnes* is a common member of the oral microflora though its role in the development of oral pathology was not widely recognized until recently (Park et al., 2024). *C. acnes* is an anaerobic, commensal Gram-positive rod (Almoughrabie et al., 2023). It inhabits various regions of the human body including the oral cavity, intestine, genitourinary tract, and skin (Cros et al., 2023). Normally, this microorganism is harmless, but can also act as an opportunistic pathogen in various diseases (Mayslich et al., 2021). It is prominently associated with the pathogenesis of acne vulgaris (Dréno et al., 2018) and infections related to orthopaedic prostheses (Boisrenoult, 2018). *C. acnes* is responsible for up to 10 % of prosthetic joint infections, most commonly infecting the shoulder joint, although the occurrence was also reported in the hip and knee prostheses (Boisrenoult, 2018). It also contributes to various ophthalmological complications such as post-operative endophthalmitis (Fowler et al., 2021), potentially influences the risk of prostate cancer via prostate inflammation (Ugge et al., 2018), can cause endocarditis in individuals with prosthetic heart valves (Patel et al., 2022) and has been occasionally mentioned in connection with Alzheimer's disease (Emery et al., 2017). In the context of oral diseases, *C. acnes* was found to have a role in secondary endodontic infections and persistent endodontic lesions (Dioguardi et al., 2020; Niazi et al., 2016). It has been found that *C. acnes* and its extracellular matrix are integrated into the oral biofilm during its formation (Kolenbrander et al., 2010). Furthermore, a recent study established a causal link between *C. acnes* and peri-implantitis (Park et al., 2024). The researchers demonstrated the almost ubiquitous presence of this microbe in the macrophages of severe peri-implant lesions (Park et al., 2024), pointing to an immune response and highlighting its role in disease development.

The slow growth rate and intricate cultivation requirements of *C. acnes* pose challenges for accurate diagnostics (Bossard et al., 2016). Furthermore, its ability to form biofilms (*in vitro* as well as *in vivo*), which were proved to be able to adhere to various metals, including titanium, contributes to the resilience of infections against therapeutic interventions (Bayston et al., 2007; Coenye et al., 2022; Garcia et al., 2020). Concerning the increasing incidence of treatment failure due to biofilm-associated resilience and antibiotic resistance, a need to explore alternative strategies to combat biofilm and multidrug-resistant strains is imperative.

By specifically targeting *C. acnes*, targeted therapies could potentially disrupt oral biofilms and prevent disease onset. Bacteriophage therapy – the therapeutic use of lytic bacterial viruses, holds significant promise as a potential approach for controlling oral biofilms. The development of bacteriophage-based treatments, which originated decades ago, was largely abandoned after the discovery of antibiotics. However, with the growing resistance of bacterial pathogens to antibiotics, this approach is once again gaining attention and could complement or even replace conventional antibiotic therapy. Phages, the most abundant entities in nature, are able to target specific bacteria. In recent years, phage therapy has been successfully applied to treat recurrent UTIs (Aslam et al., 2020), chronic rhinosinusitis (Ooi et al., 2019), prosthetic joint infections (PJI) (Tkhilaishvili et al., 2019), skin infections (Little et al., 2022), respiratory infections (Wu et al., 2021), cardiac device infections (Exarchos et al., 2020), and sepsis (Weber-Dąbrowska et al., 2003) among others. Although the oral cavity is abundant in bacteriophages, little is understood about the oral virome and its role in health or disease. Bacteriophages are typically found in environments where their bacterial hosts are present, as they rely on these bacteria for their reproduction (Hyman, 2019). This crucial relationship should be carefully considered when selecting samples for isolation efforts. For addressing biofilm-induced pathologies it is also essential that isolated therapeutic bacteriophages exhibit anti-biofilm activity. Some phages are capable of inhibiting biofilm formation, while others even possess the ability to disrupt an existing one (Domingo-Calap and Delgado-Martínez, 2018).

In the present study we aimed at isolating novel lytic bacteriophages

from saliva with the ability to disrupt formed biofilm of clinical *C. acnes* strains. When evaluating their therapeutic potential, we determined their morphology, further characterized their lytic activity, analysed their genomes and assessed their anti-biofilm activity.

## 2. Materials and methods

### 2.1. Bacterial strains

*C. acnes* DSM 1897, *Cutibacterium granulosum* DSM 20700, *Streptococcus mutans* DSM 20523 and *Streptococcus mitis* DSM 12643 were obtained from the German Collection of Microorganisms and Cell Cultures GmbH (Braunschweig, Germany). *C. acnes* NCIMB 41336 was obtained from The National Collection of Industrial, Food and Marine Bacteria (Aberdeen, UK), and *Aggregatibacter actinomycetemcomitans* NCTC 9710 was from The National Collection of Type Cultures (Salisbury, UK). 19 *C. acnes* strains were from the clinical isolates library of Valdoltra Orthopaedic Hospital, which were isolated during routine microbiological diagnostic procedures from patients undergoing revision surgery due to PJI. Species identification was performed by conventional microbiological culturing methods and confirmed by sequencing and/or using matrix-assisted laser desorption/ionization-time of flight mass spectrometry (MALDI-TOF MS; MALDI Biotyper, Bruker Daltonics, USA). All bacterial strains used in this study are listed in [Supplementary Information \(Table S1\)](#). *C. granulosum* and *C. acnes* strains were propagated on brain heart infusion (BHI) (Sigma Aldrich, USA) supplemented with 1.5 % agar (Agar Bios Special LL, Biolife, Italy) or reinforced clostridial medium (RCM) broth (Merck, Darmstadt, Germany) at 37°C in anaerobic conditions obtained with the GENbox anaer system (BioMérieux, Marcy-l'Étoile, France). *A. actinomycetemcomitans* was propagated on BHI 1.5 % agar plates with the addition of 0.5 % yeast extract (Biolife, Italy) at 37°C in CO<sub>2</sub> conditions obtained with GENbox CO 2 (BioMérieux, Marcy-l'Étoile, France). *S. mitis* and *S. mutans* were both propagated on BHI with 1.5 % agar at 37°C in aerobic conditions. *C. acnes* CA 2305 strain was used as the host for bacteriophage isolation and propagation. Its genome was fully sequenced and the absence of antimicrobial resistance genes was confirmed by running ResFinder v4.5.0 (Bortolaia et al., 2020; Camacho et al., 2009) under default parameters. For phage enrichment procedures, 2 × BHI was used. For the double agar overlay technique, a 0.7 % top agar was prepared using the same media compositions (Kropinski et al., 2009). BHI supplemented with 25 % glycerol (Sigma Aldrich, USA) was used for long-term storage at –80 °C. Bacterial strains were routinely checked by MALDI-TOF MS to rule out possible contamination.

### 2.2. Sample collection and bacteriophage isolation

Prior to saliva samples collection informed consent was obtained from all donors. The study was approved by The Ethical Committee of Valdoltra Orthopaedic Hospital (Ethics number: 7/2023) and by the National Medical Ethics Committee of the Republic of Slovenia (Ethics number: 0120–535/2023/3, 19 January 2024). The study was conducted in full accordance with the applicable principles of the Declaration of Helsinki, as revised in 2024, and all procedures followed its ethical standards (Association, 2025). Saliva samples were collected from 20 healthy donors who did not eat or brush their teeth for at least 8 h before sample collection. Because of saliva's viscosity properties, pooled samples were first diluted with two times concentrated BHI and incubated overnight at 37 °C in anaerobic conditions. After incubation, samples were centrifuged using a Sigma 3–18 KS centrifuge (Sigma Laborzentrifugen GmbH, Osterode am Harz, Germany) at 3535xg for 30 min and filtered through a 0.45 µm syringe filter (Sartorius, Germany). For phage enrichment purposes, *C. acnes* CA 2305 was cultured in BHI for 48 h in anaerobic conditions. Saliva samples were further diluted by the addition of 2 × BHI and inoculated by adding 100 µL of the prepared bacterial culture. Samples were incubated at 37 °C in

anaerobic conditions for 4 days. Enriched saliva samples were then centrifuged using Sigma 3–18KS at 3535 x g for 10 min and filtered through a 0.22 µm syringe filter (Sartorius, Germany) to remove the remaining bacteria. The presence of bacteriophages was confirmed by performing the spot assay (Kropinski et al., 2009). Briefly, bacterial lawns were prepared by inoculating melted 0.7 % BHI top agar with 300 µL of 48 h old *C. acnes* CA 2305 bacterial culture, pouring it over a BHI agar culture plate and allowing it to solidify. 10 µL of the enriched saliva samples were then spotted onto the bacterial lawn and incubated for 48 h at 37 °C in anaerobic conditions. Plates were then screened for the presence of lysis zones or single plaques, which were then picked for further single plaque purification and propagation of bacteriophages using the double agar overlay plaque assay (Bonilla et al., 2016; Kropinski et al., 2009).

To obtain a pure lysate for sequencing, single plaque purification was performed three times by picking a single phage plaque, transferring it to 200 µL of saline magnesium (SM) buffer (50 mM Tris-Cl, pH 7.5, 100 mM NaCl, 8 mM MgSO<sub>4</sub>, 0.01 % (w/v) gelatin) and leaving it at 4 °C overnight to allow phages to diffuse from the agar into the SM buffer. Then, the SM buffer with phages were centrifuged at 9000 x g for 10 min using a MiniSpin® plus tabletop microcentrifuge (Eppendorf, Netherlands) to remove bacteria and agar. Ten-fold serial dilutions of were prepared using the supernatant and plaque assay was performed to get single plaques for the next purification round. Throughout the purification process, plaque morphology was meticulously examined.

After the single plaque purification process, phages were propagated using the double agar overlay plaque assay (Kropinski et al., 2009) with *C. acnes* CA 2305 as their host strain. 5 mL of SM buffer was added to each plate with confluent lysis of host lawns. Plates were incubated at room temperature in anaerobic conditions with gentle shaking for 4 h. The SM buffer containing phages was carefully aspirated from plates, centrifuged using Sigma 3–18KS at 8512 x g for 15 min, and filtered through a 0.22 µm syringe filter. Phage lysates were stored at 4 °C until used. Phage titer was determined by the double agar overlay plaque assay (Kropinski et al., 2009).

### 2.3. Phage DNA extraction and sequencing

Phage DNA from phage lysates was extracted using an adapted phenol-chloroform extraction method. First, 5xPEG (20 % PEG-6000 (Fisher Scientific, USA), 2.5 M NaCl (Carlo Erba Reagents GmbH, Milano, Italy)) was added to phage lysates at a ratio of 1:4 precipitant: lysate, and mixed gently by inversion. Mixtures were incubated at 4 °C overnight to allow for phage precipitation. Then, samples were centrifuged at 4 °C using Sigma 3–18KS, first at 10,000 x g for 30 min, followed by a 11,000 x g centrifugation for an additional 30 min. Pellets were resuspended in 5 mM MgSO<sub>4</sub> (Carl Roth, Karlsruhe, Germany) by gentle pipetting. Contaminating bacterial nucleic acids were removed by treating the samples for 1 h at 37 °C with DNase (1 U/µL, Thermo Fisher Scientific, USA) and RNase (10 mg/mL, Thermo Fisher Scientific, USA). DNase deactivation was carried out by the addition of EDTA (Sigma-Aldrich, USA) pH 8.0 at a final concentration of 5 mM for 10 min at 65 °C. To open phage capsids, a mixture of Proteinase K (Thermo Fisher Scientific, Massachusetts, USA) at a final concentration of 1 mg/mL, SDS (Sigma-Aldrich, USA) at a final concentration of 0.5 %, and EDTA pH 8.0 at a final concentration of 20 mM was added and samples were incubated for 1 h at 60 °C. Then, an equal volume of phenol:chloroform: Isoamyl alcohol (25:24:1) (Sigma Aldrich, USA) was added and samples were centrifuged using a MiniSpin® plus centrifuge at 3000 x g for 5 min. This was repeated one more time. At that point, an equal volume of chloroform (Honeywell Riedel-de Haen, USA) was added and samples were centrifuged again. For DNA precipitation, 3 M NaOAc (pH 5.2, Sigma-Aldrich, USA) at a 1:10 vol ratio and 2.5 volumes of 96 % ice-cold ethanol (Valdoltra Orthopedic Hospital Pharmacy, Ankaran, Slovenia) were added and samples were incubated at –20 °C overnight. Next, samples were centrifuged using a Sigma 3–18KS centrifuge for 20 min at

12,500xg. Pellets were washed with 80 % ethanol and centrifuged using MiniSpin® plus centrifuge at max speed for 2 min. This was repeated twice. Ethanol was removed without disturbing the pellets and tubes were left to dry for 30 min. DNA was dissolved in dH<sub>2</sub>O (Invitrogen, USA). Phage DNA concentrations were determined using a Qubit Fluorometric Quantification device (Thermo Fisher Scientific, Massachusetts, US). The DNA quality control, the in vitro fragment library preparations (paired-end libraries) and Illumina NovaSeq sequencing were carried out by SeqOmics Biotechnology Ltd. (Mórahalom, Hungary). Obtained reads were submitted to The Bacterial and Viral Bioinformatics Resource Center' (BV-BRC) assembly service and were assembled using Unicycler v0.4.8 (Wick et al., 2017). Quast v5.2.0 (a quality assessment tool) was used to evaluate the quality of genome assemblies (Gurevich et al., 2013). PhageTerm (Garneau et al., 2017) was used to locate phage termini and reorder the genomes accordingly when needed. Contigs were annotated using PROKKA (Seemann, 2014), MetaGeneAnnotator (Noguchi et al., 2008), and PHANOTATE (McNair et al., 2019). Putative protein functions were analysed and annotated by searching against the nonredundant protein database with BLASTp (Altschul et al., 1997).

### 2.4. Comparative genomic analyses

The complete genomes of *Cutibacterium* phage Corretto and Ristretto were compared with other phage genome sequences available in the nr/nt NCBI database using BLASTn (Camacho et al., 2009) (accessed on October 17th 2024). Genomes of phages showing a percental identity equal to or higher than 92 % were selected and their sequences in FASTA format were downloaded from the database. The pairwise intergenomic similarities amongst 38 phage genomes from the GenBank database and phages Corretto and Ristretto were computed using the Virus Intergenomic Distance Calculator, VIRIDIC (Moraru et al., 2020), under default settings (species similarity threshold: 95 %; Genus similarity threshold: 70 %). A proteomic tree of viral genome sequences of phages Corretto and Ristretto and other related prokaryotic dsDNA virus genome sequences were generated based on genome-wide sequence similarities computed by tBLASTx using The Viral proteomic tree server (ViPTree (Nishimura et al., 2017)) version 4.1 (accessed on October 17th 2024). Alignments of closely related genomes were visualised through The Dynamic Genomic Alignment sever (DiGAlign (Nishimura et al., 2024) version 2.0 (accessed on October 17th 2024) by generating amino acid- (tBLASTx) resolved alignments.

The nucleotide database of GenBank (Sayers et al., 2019) was searched for *Cutibacterium* (former *Propionibacterium*) phage genomes that have been sequenced to date. The search query was as follows: “(((Propionibacterium[Title]) OR *Cutibacterium*[Title]) AND phage [Title]) AND complete[Title]) AND genome[Title]”, aiming only at complete genomes (accessed on October 24th 2024). The list of hits was manually checked for doubled genomes, and remaining genome sequences were downloaded from the database in FASTA format and submitted to VIRIDIC. The pairwise intergenomic similarities were computed under default settings, to determine the number of unique *Cutibacterium* phages in the database.

### 2.5. Phage morphology examination with transmission electron microscopy (TEM)

Samples for TEM analysis were prepared using negative staining with 2 % phosphotungstic acid (PTA). Samples were gently mixed and applied to copper grids, incubated for 5 min, washed, and contrasted with a drop of 1 % aqueous solution of uranyl acetate (UA). Two grids were prepared for each sample. Phage morphology was examined using TALOS L120 scanning electron microscope (Thermo Fisher Scientific, USA) at the accelerating voltage of 120 kV.

## 2.6. Host range determination

Host ranges of isolated phages were determined by the double agar overlay method (Kropinski et al., 2009) and spot assay (Kutter and Sulakvelidze, 2004). All bacterial strains used for host range determination are listed in Supplementary Information (Table S1). On bacterial lawns where lysis was observed, the relative efficiency of plating (EOP) was calculated as the phage titer on the tested strain divided by the titer on the phage host strain. All experiments were conducted in triplicates.

## 2.7. Biofilm formation and phage anti-biofilm activity assessment

First, the biofilm formation ability of *Cutibacterium* spp. strains (Table S1) were assessed. 3–5 colonies of each strain were used to inoculate 3 mL of RCM growth media and incubated at 37°C under anaerobic conditions for 72 h. The bacterial inoculum for biofilm formation was prepared by diluting the liquid cultures 100 × in RCM. 200 µL of the bacterial inoculum per well was used to seed the tissue-culture-treated 96-well plates. Plates were incubated at 37 °C under static anaerobic conditions obtained with the GENbox anaer system (BioMérieux, Marcy-l'Étoile, France) and biofilm formation was allowed to proceed for 72 h. A *C. acnes* strain (CA 2001) that exhibited minimal or undetectable biofilm formation under in vitro conditions (as assessed by the crystal violet assay) was included as a negative control for biofilm formation. For sterility control, wells with 200 µL of RCM were also included. Biofilm quantification was performed with the crystal violet method. Briefly, wells were rinsed 3 × with 220 µL of PBS buffer (Gibco, Thermo Fisher Scientific, USA) to remove non-adherent bacteria and allowed to dry at room temperature. Wells were then treated with 220 µL of 99 % methanol (Honeywell Riedel-de Haen, USA) for 20 min for biofilm fixation. Following methanol removal and drying, 220 µL of 0.1 % crystal violet solution (Sigma Aldrich, USA) was added to the wells for 15 min biomass staining. Excess dye was washed away with distilled water. After drying, the crystal violet dye bound to biofilms was dissolved by the addition of 220 µL 33 % acetic acid (Carlo Erba Reagents GmbH, Milano, Italy) for 30 min. 200 µL of the solution was transferred to a fresh 96-well plate and biofilms were quantified measuring the optical density of the crystal violet at 595 nm using the Tecan Infinite 200 Pro M Plex plate reader. The experiment was performed two times with five technical replicates.

Seven strains with high biofilm formation ability were selected for the assessment of phage's anti-biofilm activity. First, bacterial biofilms were formed as already described. After that, wells were washed 1 × with PBS. 180 µL of fresh RCM media and 20 µL of phage suspension were added per well. Phages were assessed for their antibiofilm activity at three different concentrations:  $5.7 \times 10^8$  PFU/mL,  $5.7 \times 10^7$  PFU/mL and  $5.7 \times 10^6$  PFU/mL. For negative control wells, 200 µL of RCM media was added to biofilms. Sterility control wells containing only RCM media (no biofilm) and only phage suspensions were also included in each experiment. Plates were incubated in static anaerobic conditions for 72 h. Biofilm biomass was quantified with the crystal violet method as already described. Experiments were performed three times with seven technical replicates. A decrease in biofilm biomass equal or higher than 97 % was considered as complete biofilm eradication.

## 2.8. Statistical analysis

Data obtained from biofilm formation and phage disruption were presented in the form of vertical box plots with individual data points and statistically analysed using SigmaPlot 15.0 (Systat Software, Chicago, IL, USA). The normality of data distribution was assessed with the Shapiro–Wilk test. If data were not normally distributed or the equal variance test failed, the nonparametric Kruskal–Wallis test was performed followed by the Dunnett's post hoc test for multiple comparison versus the control group and by the Student–Newman–Keuls post hoc test for all pairwise multiple comparison between different phage treatment

groups. To determine the statistical difference between biofilm forming bacteria, the non-biofilm former strain represented the control group. To determine phage anti-biofilm activity, the non-treated biofilm represented the control group. Statistical significance was determined as  $P < 0.05$ .

## 3. Results

### 3.1. Bacteriophage isolation, sequencing and genome analysis

Saliva samples collected from 20 healthy donors were processed and screened on *C. acnes* CA 2305 lawn, revealing 9 distinct single plaque formations. Some plaques had different morphologies, indicating the possible existence of a diverse phage community. After the single plaque purification process, all 9 isolates were propagated and phage DNA was extracted. Sample sequencing and genome analysis revealed two new lytic bacteriophages. The genome sequences have been deposited in GenBank under accession numbers PP165414 (phage Ristretto) and PP238470 (phage Corretto).

The complete genomes of phage Ristretto and phage Corretto comprised 28,996 base pairs (bp) and 29,507 bp, with G+C contents of 54.20 % and 54.00 %, respectively. 40 protein coding sequences (CDS) were identified in phage Ristretto genome. The annotation included 11 hypothetical proteins and 29 proteins with functional assignments. In the phage Corretto genome, 42 CDS were identified and the annotation included 9 hypothetical proteins and 33 proteins with functional assignments. Identified coding sequences were associated with phage structure, host lysis, DNA packing, and replication. No integration, recombination, virulence, or antimicrobial resistance genes were found, making them suitable for possible therapeutic use.

The search of the nucleotide database of GenBank returned 230 hits for complete *Cutibacterium* (*Propionibacterium*) phage genomes. After manually revising for doubled hits, a total of 153 bacteriophages remained and were submitted to VIRIDIC (Supplementary Information – excel file). 51 bacteriophages were found to have a high intergenomic similarity ( $\geq 95$  % genome-wide nucleotide identity) with at least 1 of the other phages, leaving 102 unique phages. 9 phages had no or very little intergenomic similarities with the other 93 phages, and belonged to the group of phages infecting *Propionibacterium freudenreichii*. The other 93 phages were *Cutibacterium acnes* phages with genomes in the size range from 28,876 (phage Attacne, accession number KR337651.1) to 30,112 (phage Aquarius, accession number MF919491.1) bp (Supplementary Information: Figure S1).

The pairwise intergenomic similarities amongst *Cutibacterium* (*Propionibacterium*) phage genomes from the GenBank database was computed using VIRIDIC (Supplementary Information: Figure S2) and revealed that phage Corretto had the highest intergenomic similarity with *Propionibacterium* phage P100D (accession number JX262220.1) – 92.041 % and phage Ristretto had the highest intergenomic similarity with *Propionibacterium* phage P105 (accession number JX262219.1) – 91.873 %. The intergenomic similarity between phages Corretto and Ristretto was 90.144 %. Results indicate that phages Corretto and Ristretto represent new species within the genus *Pahevavirus*, from the class *Caudoviricetes* (Fig. 1).

### 3.2. Morphological analysis and host range determination

Phages were morphologically analysed by transmission electron microscopy. Visualised bacteriophages belonged to the *Caudoviricetes* class, morphologically corresponding to the *siphovirus* group. They had an icosahedral head of about 50 nm in diameter and a long, flexible tail of about 150 nm ending with short attachment fibrils (Fig. 4, A and B).

The host range of phages was evaluated on 25 different clinical and reference strains. Both phages showed high specificity for *C. acnes*, and were unable to lyse other tested bacterial strains or species. Phage Ristretto lysed 11 out of 21 *C. acnes* strains and displayed higher EOPs (all

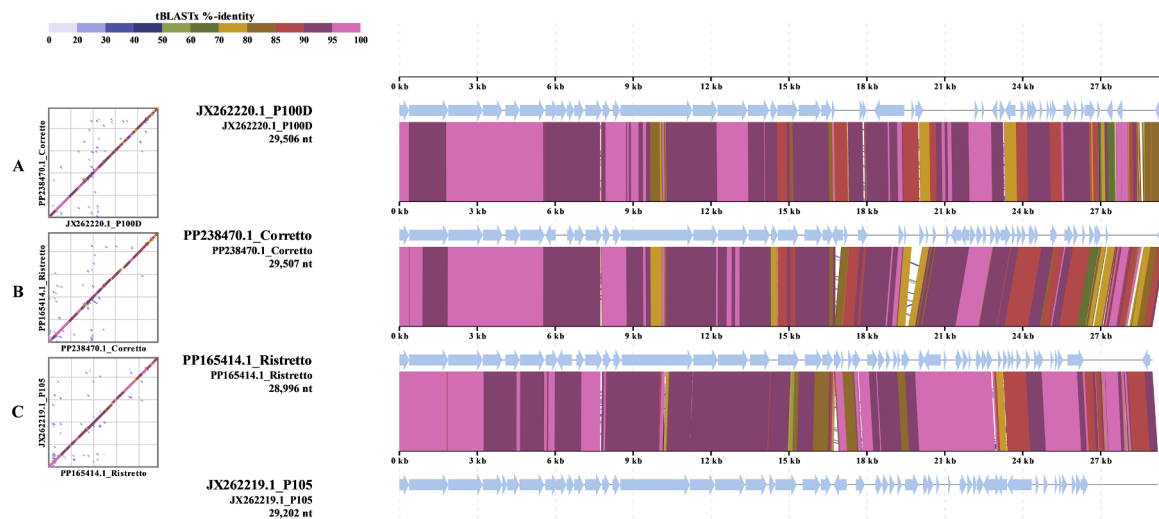


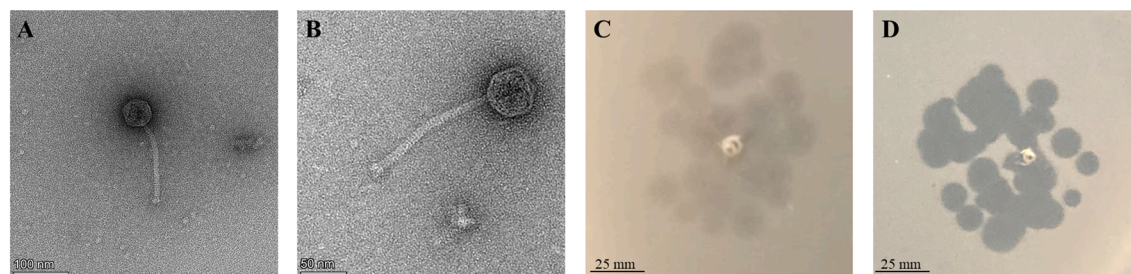
**Fig. 1.** Whole genome alignments of phages Corretto and P100D (A), phages Corretto and Ristretto (B) and phages Ristretto and P105 (C). A whole genome comparison was performed using tBLASTx on the DiGAlign server. High-similarity regions are color-coded on the basis of the tBLASTx percentage identity and dot plot charts summarize these regions.

equal or above 0.999), while phage Corretto displayed a broader host range, specifically lysing 17 out of 21 *C. acnes* strains but with 8 EOPs below 0.001. Plaque morphology varied from clear to turbid with hazy edges (Fig. 2).

**3.3. Biofilm formation and phage antibiofilm activity**

Twenty-one *C. acnes* strains and a *C. granulosum* (DSM 20700) strain

were assessed for their ability to form biofilm. Seven *C. acnes* strains demonstrated high biofilm formation ability compared to the control non-biofilm former strain *C. acnes* CA 2001 ( $P < 0.001$ ). The amount of their total biofilm biomass was 7.4–15.2 × the amount of the control strain (based on groups median values). Two *C. acnes* strains exhibited medium ( $P < 0.01$ ) and two low ( $P < 0.05$ ) biofilm formation capability. The amount of their total biofilm biomass was 1.7–1.8 × the amount of the control strain in medium biofilm formers and 0.8 × in low



**E**

EOP ≥ 1.000
EOP 0.100 – 0.999
EOP 0.010 – 0.099
EOP 0.001 – 0.009
EOP < 0.001
No lysis

	CA 2305 (host)	CA 1301	CA 2001	CA 2101	CA 2102	CA 2103	CA 2104	CA 2105	CA 2201	CA 2202	CA 2203	CA 2204	CA 2205	CA 2206	CA 2207	CA 2301	CA 2302	CA 2303	CA 2304	NCIMB 41336	DSM 1897	<i>C. granulosum</i> DSM 20700	<i>A. actinomycetemcomitans</i> NCTC 9710	<i>S. mutans</i> DSM 20523	<i>S. mitis</i> DSM 12643
Bacteriophage Ristretto	c		c				t	t	c					c	c	t	c		t		c				
Bacteriophage Corretto	c		c	t	t	t	t	c	c	t	t	t		c	c	c	t		c		t				

**Fig. 2.** Phage phenotypical characteristics: phage and plaque morphology, host range, and EOP. Transmission electron microscopy images show *Cutibacterium* phage Ristretto (A) and *Cutibacterium* phage Corretto (B) morphology. Representative pictures of plaque morphologies (C; turbid and D; clear) are given as an example. The host range (E) assessed against 25 bacterial strains is presented by different colours, depending on the obtained efficiency of plating (EOP). Plaque morphology in the table is marked t as turbid or c as clear for each strain. Photographs provided by the authors.

biofilm formers. The remaining 11 *Cutibacterium* strains did not form biofilms (Fig. 3).

Phages' antibiofilm ability was tested against *C. acnes* strains with high biofilm formation ability. Based on its host range, phage Corretto was assessed against biofilms of all 7 *C. acnes* strains with high biofilm formation ability, whereas phage Ristretto was assessed only against biofilms of *C. acnes* strains CA 1301, CA 2104 and CA 2302.

Both phages completely eradicated the biofilm of CA 2302 ( $\geq 97\%$ ). Phage Ristretto decreased the biofilm biomass of strain CA 2302 by 99.4% (OD600 0.06) when used at the concentration of  $10^8$  PFU/mL and by 97% (OD600 0.31 and 0.32; median values) when used in concentrations of  $10^7$  PFU/mL and  $10^6$  PFU/mL, respectively (Fig. 4, A). Similarly, phage Corretto decreased the biofilm biomass of the same strain by 98.3–99.5% (OD600 0.03–0.04; median values) at all tested phage concentrations (Fig. 4, B). Phage Ristretto decreased the biofilm biomass of CA 2104 by 14% when applied at the highest concentration. At the concentration of  $10^7$  PFU/mL no statistically significant difference was observed compared to the non-treated control ( $P = 0.214$ ). At the concentration of  $10^6$  PFU/mL, the biofilm appeared to even increase in biomass by 14% (Fig. 5, A). Similar observations were made with phage Corretto. Phage Corretto almost completely (by 94%) eradicated the biofilm of CA 2104 when applied at the highest ( $10^8$  PFU/mL) concentration (Fig. 5, B). Surprisingly, phage showed no effect on biofilm ( $P = 0.946$ ) at a 10x lower concentration, and at the concentration of  $10^7$  PFU/mL, the biofilm appeared to even increase in biomass by 28%.

When applied to the biofilm of CA 1301 (Fig. 6, A), phage Ristretto significantly ( $P < 0.001$ ) decreased biofilm biomass at all three concentrations, with the most effect observed at  $10^8$  PFU/mL (45%), whereas there was no statistical difference between the use of  $10^7$  PFU/mL and  $10^6$  PFU/mL phage concentration (28–32%;  $P = 0.141$ ). When phage Corretto was applied to CA 1301 biofilm at  $10^8$  PFU/mL, it lowered the biofilm by 45%, at  $10^7$  PFU/mL by 32%, and at  $10^6$  PFU/mL by 28%. The differences between the treatment groups and control group were all statistically significant ( $P < 0.001$ ) (Fig. 6, B).

Phage Corretto decreased the biofilm biomass of CA 2202 (Fig. 7, A) by 98.5–99.5% (OD600 0.07–0.20; median values), at all tested phage concentrations, which was considered a complete biofilm eradication. Whereas the biofilm biomass of CA 2101 decreased by 56–66% at all phage Corretto concentrations with no statistically significant difference between treatment groups ( $P = 0.505$ – $0.980$ ) (Fig. 7, B). No statistically

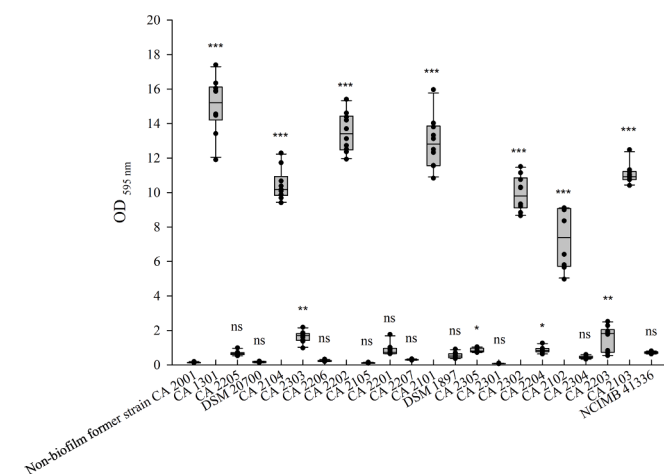


**Fig. 3.** Biofilm formation of 22 *Cutibacterium* strains. *C. acnes* CA 2001 represents the negative control as a non-biofilm former (strain that exhibited minimal or undetectable biofilm formation under in vitro conditions). Multiple comparisons versus non-biofilm former control strain were performed with Dunnett's method: ns, not statistically significant – no biofilm formation ability; \* $P < 0.05$ , low biofilm formation ability; \*\* $P < 0.01$ , medium biofilm formation ability and \*\*\* $P < 0.001$ , high biofilm formation ability.

significant decrease in biofilm biomass was observed when phage Corretto was applied to CA 2102 (Fig. 7, C) and CA 2103 (Fig. 7, D) biofilms.

#### 4. Discussion

The main aim of our study was to isolate novel lytic bacteriophages with the ability to disrupt biofilm of *C. acnes* strains and to evaluate their therapeutic potential for oral biofilms biocontrol. While *C. acnes* phages are predominantly isolated from skin (mostly from patients with acne vulgaris), they can also be detected in saliva and sewage samples (Brown et al., 2016; Han et al., 2023; Liu et al., 2024; Rimón et al., 2023; Xuan et al., 2023). As our goal was to isolate bacteriophages to specifically target oral biofilms, we first wanted to confirm their presence in the oral cavity. After isolation protocol optimisation, we successfully isolated two novel lytic bacteriophages from saliva samples of 20 healthy donors that target *C. acnes* and effectively reduce mature biofilms formed by the tested clinical bacterial strains.

During biofilm disruption assay, both, phage Corretto and phage Ristretto, showed promising results in *C. acnes* biofilm reduction, with phage Corretto performing better and being effective against a wider spectrum of *C. acnes* strains. Similarly, a novel *C. acnes* phage vB\_CacS-HV1, recently isolated from saliva, exhibited a significant reduction of mature *C. acnes* biofilm and inhibited biofilm formation (Li et al., 2024). Interestingly, varying concentrations of phage vB\_CacS-HV1 produced the same antibiofilm activity, whereas our study found the activity of phages Corretto and Ristretto to be dosage-dependent.

Although biofilms are composed of a complex extracellular matrix—including polysaccharides, proteins, extracellular DNA, and lipids—that can act as a barrier to phage penetration, several bacteriophages have evolved mechanisms to overcome this defense. Notably, some phages encode extracellular polysaccharide-degrading enzymes (e.g., depolymerases), which enable them to penetrate and disrupt biofilm matrices, thereby increasing access to embedded bacterial cells (Pires et al., 2016). In our study, phage treatment led to a marked reduction in the biofilm biomass of some *C. acnes* strains, suggesting that the phages were able to at least partially penetrate the biofilm matrix to reach and lyse bacterial cells and/or disrupt components of the matrix through enzymatic or indirect mechanisms. Although we did not investigate the presence or activity of specific depolymerases in this work, we recognize this as a key direction for future research. As the molecular mechanisms of phage-mediated biofilm disruption remain underexplored in *C. acnes*, future studies should aim to characterize phage–biofilm interactions in more detail, including the role of virion-associated enzymes in matrix degradation.

Additionally, our study primarily used crystal violet staining to quantify reductions in biofilm biomass following phage treatment. Additional analyses—such as quantification of viable bacteria (CFUs) and high-resolution imaging—would further substantiate the antibiofilm effects observed. However, CFU enumeration after phage exposure presents technical challenges, particularly due to residual phages that may continue to infect and lyse bacteria during or after biofilm disruption, potentially leading to underestimation of viable counts. Future studies should incorporate phage-neutralizing steps or virucidal agents to enable accurate CFU assessment post-treatment. Additionally, visualizing biofilm architecture before and after phage exposure using techniques such as fluorescence microscopy (Bai et al., 2023), confocal laser scanning microscopy (Winans et al., 2022), or scanning electron microscopy (Talank et al., 2022) would provide qualitative insights into matrix disruption and cell lysis, and further support the potential of these phages as anti-biofilm agents.

Although phages Corretto and Ristretto successfully infected the tested biofilm-forming bacteria during host range assays, they were ineffective in reducing the biofilms of certain strains. Observed differences in biofilm reduction from strain to strain—particularly the strong effect seen in strain 2302—may be influenced by strain-specific variation in biofilm morphology or matrix composition. These differences

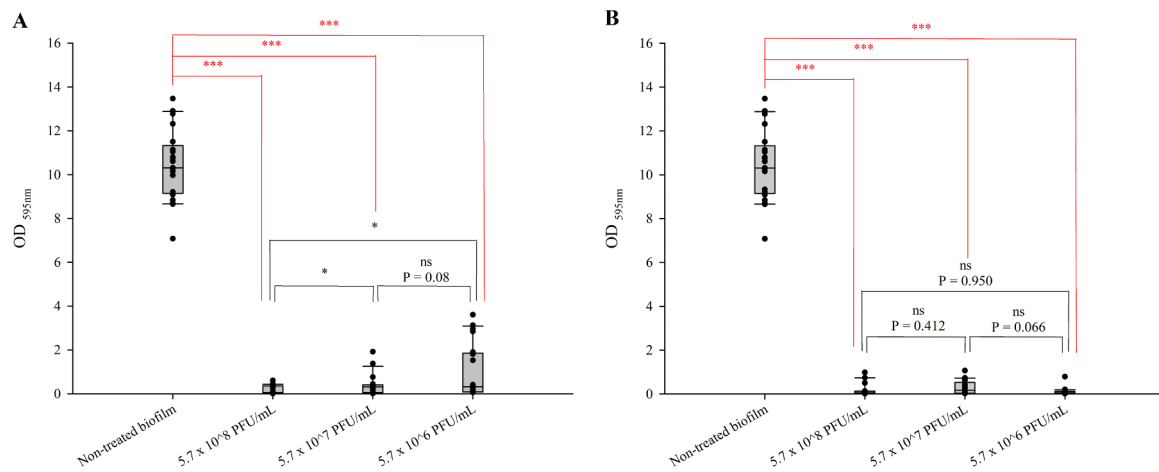


**Fig. 4.** Phage Ristretto's (A) and phage Corretto's (B) anti-biofilm activity on *C. acnes* CA 2302 biofilm. In red, multiple comparisons versus non-treated control with Dunnett's method. In black, all pairwise multiple comparison procedures with the Student-Newman-Keuls method. \*\*\*,  $P < 0.001$ ; \*  $< 0.05$ ; ns, not statistically significant.

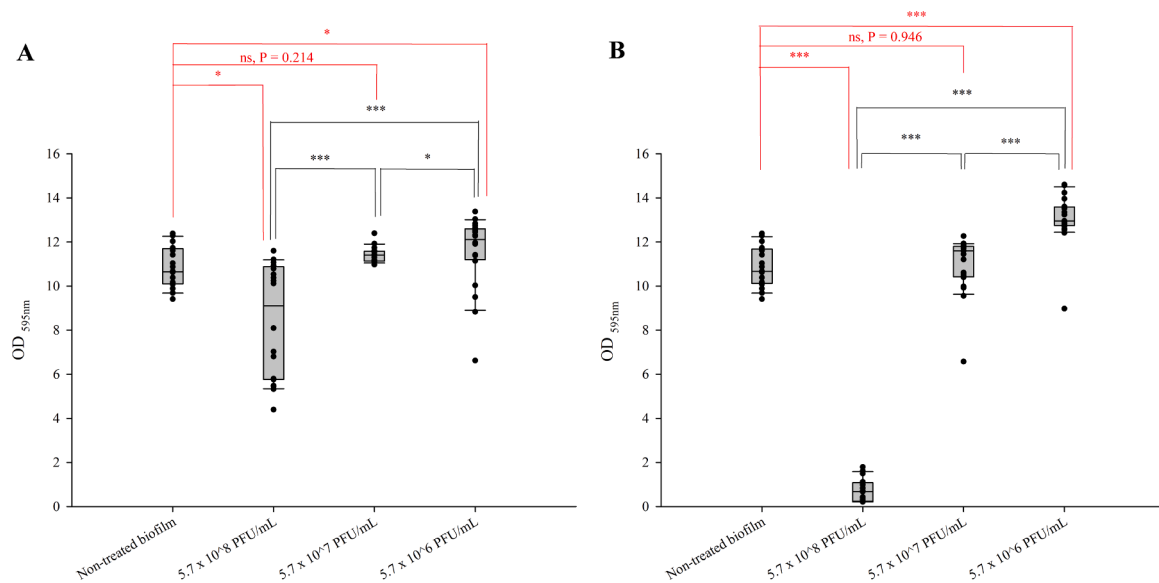


**Fig. 5.** Phage Ristretto's (A) and phage Corretto's (B) anti-biofilm activity on *C. acnes* CA 2104 biofilm. In red, multiple comparisons versus non-treated control with Dunnett's method. In black, all pairwise multiple comparison procedures with Student-Newman-Keuls method. \*\*\*,  $P < 0.001$ ; \*  $< 0.05$ ; ns, not statistically significant.

could reflect varying densities, adherence properties, or susceptibility to phage-mediated disruption. Those bacterial strains may possess defence mechanisms against phage that are specifically expressed only in biofilm settings, which can involve quorum sensing (QS), a bacterial communication system that regulates gene expression in response to population density changes. QS can modulate the expression of phage receptors or increase the production of the biofilm matrix, thereby enhancing bacterial resistance to phage (Høyland-Kroghsbo et al., 2013). This means that bacteria can modify or mask surface receptors, deploy CRISPR-Cas systems to recognize and degrade phage DNA, and produce extracellular vesicles to bind phages or extracellular matrices to block phage access (Pires et al., 2021). Additionally, studies have shown that the coexistence of phage-resistant and susceptible bacterial populations within biofilms can result in structured biofilms where phage-resistant cells can shield susceptible bacteria (Simmons et al., 2020). Variations in the impact of a single bacteriophage on a specific *C. acnes* biofilm could also result from differences in biofilm formation strength (so called “bridging”) among individual bacterial cells (Das et al., 2014) and

alternatively even slower metabolic rate of some bacteria in the biofilm, which could slow down the phage's lytic cycle (Geng et al., 2024).

Variations in biofilm reduction between tested phages were observed when applied on preformed biofilms of same strains. This could suggest that phage Corretto and Ristretto employ different mechanisms against biofilm, or that Corretto had evolved more efficient adaptations that resulted in a better antibacterial and antibiofilm activity. In fact, phages can undergo mutations that enable overcoming bacterial defence mechanisms by evolving new ways to bind to modified receptors, evading CRISPR-Cas systems, or degrading the biofilm (Egido et al., 2022). This phage adaptability in antibacterial properties' enhancement is the base principle of “phage training”, where the evolution of more effective phage variants is encouraged for phage therapy, with the emphasis on overcoming bacterial resistance, broadening the host range, and enhancing the infectivity of a potentially therapeutic phage (Ngiam et al., 2024). To overcome bacterial resistance to a single phage, phage cocktails are also in use (Kim et al., 2024) and we believe that the performance of phages Ristretto and Corretto could be enhanced by

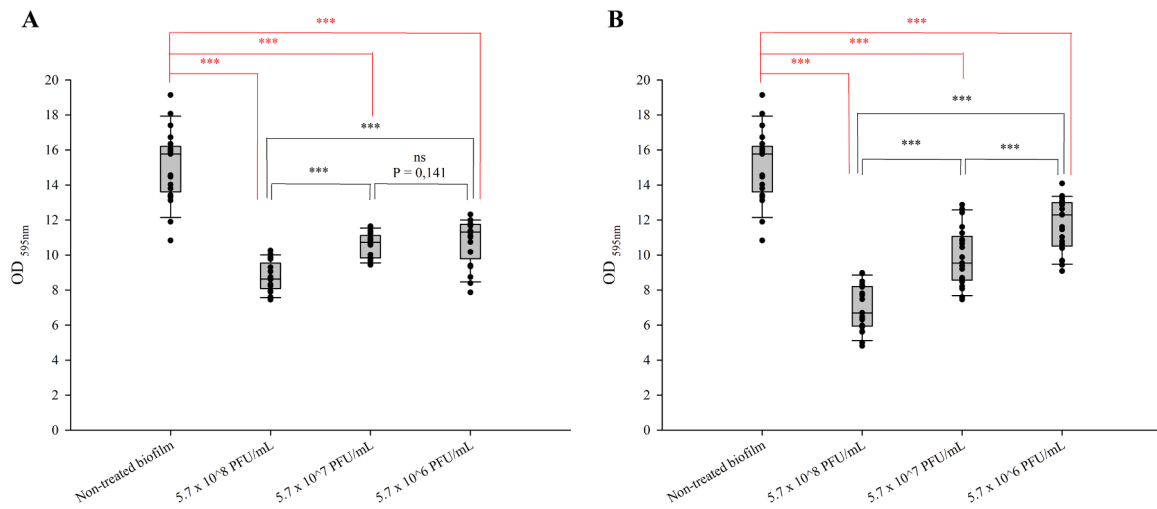


Fig. 6. Phage Ristretto's (A) and phage Corretto's (B) anti-biofilm activity on *C. acnes* CA 1301 biofilm. In red, multiple comparisons versus non-treated control with Dunnett's method. In black, all pairwise multiple comparison procedures with the Student-Newman-Keuls method. \*\*\*,  $P < 0.001$ ; ns, not statistically significant.

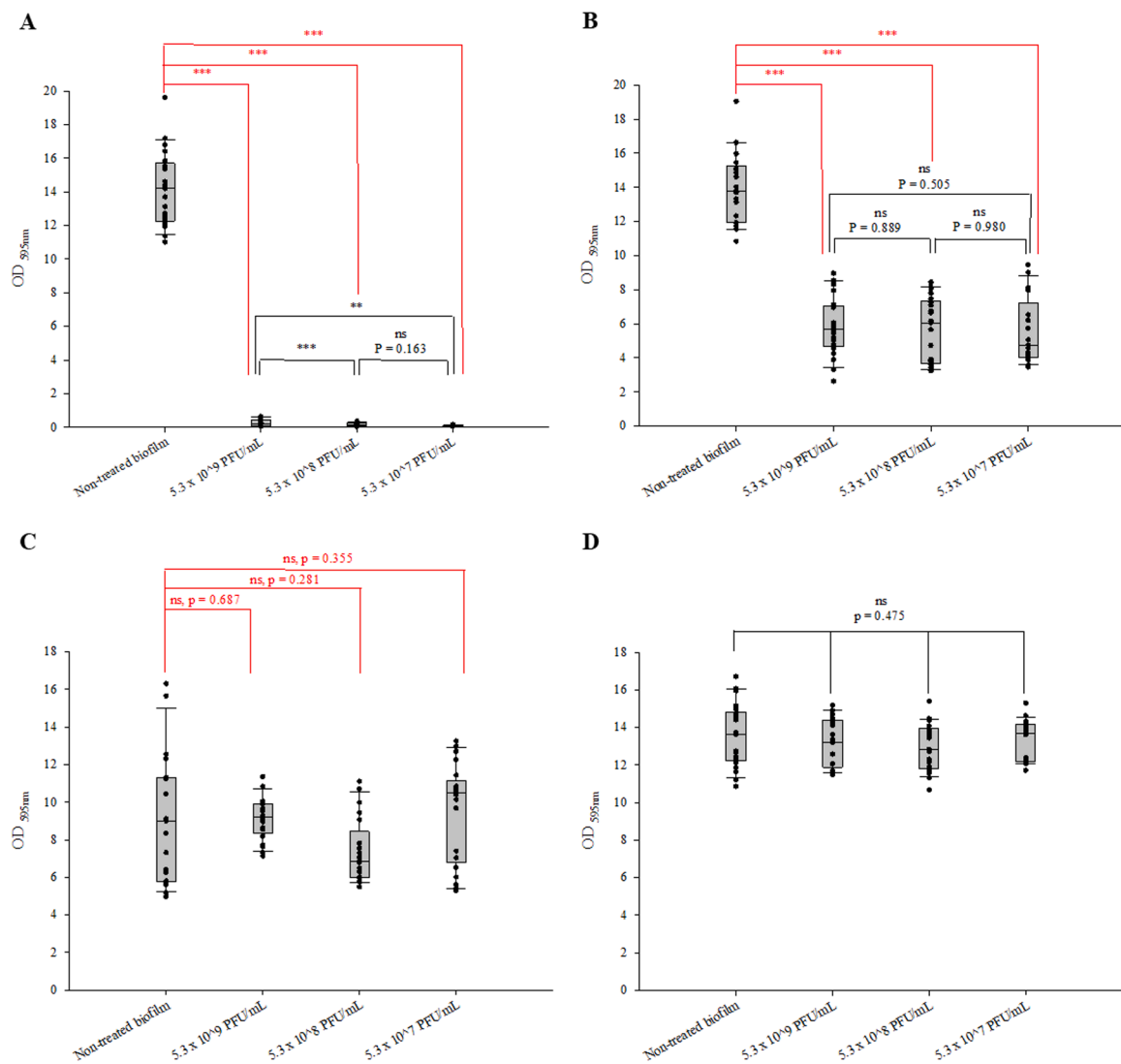


Fig. 7. Phage Corretto's anti-biofilm activity against *C. acnes* strains: CA 2202 (A), CA 2101 (B), CA 2102 (C), and CA 2103 (D). In red, multiple comparisons versus non-treated control with Dunnett's method (A, B, and C). In black, all pairwise multiple comparison procedures with the Student-Newman-Keuls method (A and B). The differences in the median values among the treatment groups (D) are not statistically different with Kruskal-Wallis One Way Analysis of Variance on Ranks ( $P = 0.475$ ). \*\*\*,  $P < 0.001$ ; \*\*  $< 0.01$ ; ns, not statistically significant.

combining them against biofilm. To confirm that, further studies including phage compatibility, synergistic and possible antagonistic effects would have to be performed in the future. Some recent studies offer optimistic evidence of synergistic effects with *C. acnes* phage combinations, however only a handful tested their antibiofilm activity. Chen et al. (Chen et al., 2024) isolated nine *C. acnes* phages from human skin and evaluated their antibiofilm activity on titanium discs. They chose 4 strains of *C. acnes* with best biofilm formation capabilities and observed a significant reduction in bacterial counts by using a combination of 4 selected phages with the broadest host range.

Phages Corretto and Ristretto were found to specifically infect *C. acnes* strains, exhibiting a relatively broad host range. Notably, phage Corretto demonstrated greater efficacy, lysing six more *C. acnes* strains than phage Ristretto. According to literature, a broad spectrum activity is typical for *C. acnes* bacteriophages (Marinelli et al., 2012). Recent studies reinforce these findings. For instance, the newly isolated phages Y3Z (Xuan et al., 2023), TCUCAP1 (Lam et al., 2021) and  $\phi$ PaP11-13 (Liao et al., 2023) have all demonstrated similar results. In a study by Kim et al. (Kim et al., 2022), 15 *C. acnes* phages exhibited a broad host range. Similarly, Rimon et al. (Rimon et al., 2023) reported that 88 % of the eight *C. acnes* phages they analysed displayed a wide host range. Another study further confirmed this trend, showing extensive host range capabilities in all three selected *C. acnes* phages (Golebo et al., 2022). The shared feature of *C. acnes* phages is likely due to their high genetic similarity. This characteristic is a significant advantage, as a bacteriophage's therapeutic potential relies not only on being strictly lytic but also on having a broad host range to effectively target multiple harmful strains (Hyman, 2019). On the other hand, specificity to a single species is advantageous, as our goal is to selectively target and eliminate harmful bacteria within polymicrobial biofilms while preserving the beneficial symbiotic microbes that sustain a balanced microbial environment. In fact, phages Corretto and Ristretto were unable to infect other tested bacterial species involved in the oral biofilm, such as *Streptococcus mutans* and *Streptococcus mitis*, or other strains of *Cutibacterium* spp. These observations align with findings from previous studies (Brown et al., 2016; Golebo et al., 2022; Kim et al., 2022).

Another notably shared characteristic of *C. acnes* bacteriophages is their morphology, which corresponds to the Siphoviridae family. Same morphology characteristics were observed in phages Corretto and Ristretto, consistent with findings reported in previous studies (Kim et al., 2022; Lam et al., 2021; Liao et al., 2023; Rimon et al., 2023; Xuan et al., 2023).

After a survey and comparative genomics analyses of completely sequenced *Cutibacterium* (*Propionibacterium*) phage genomes deposited in the nucleotide database of GenBank, identified genomes were found to be genetically similar (intergenomic similarity  $\geq 82.08$ ), except for nine phages with an exceptionally lower intergenomic similarity (0 – 0.87) to other analysed phages, that belonged to the group of phages infecting *Propionibacterium freudenreichii*. *P. freudenreichii* is used in the dairy industry for the production of Swiss cheeses (e.g. Emmentaler) (Cheng et al., 2018) and in the production of vitamin B12 and propionic acid (Wang et al., 2014). These bacteriophages exhibit a significantly greater genetic diversity than *C. acnes* bacteriophages, more narrow host ranges and potential for lysogenic replication (Cheng et al., 2018). Phages B5 and Philemon are even morphologically different, being filamentous phages with small, only about 5.8k base pair genomes (Chopin et al., 2002). Our findings are therefore in accordance with existent literature on *C. acnes* phages, which reports a significant phylogenetic similarity between *C. acnes* phages with not much of genetic diversity (Liu et al., 2015). Since the intergenomic similarities between the isolated phages Corretto and Ristretto and their closest related phages were only 92.041 % and 91.873 %, respectively, they should be considered members of two distinct species within the genus Pahexavirus, in accordance with the guidelines established by the International Committee on Taxonomy of Viruses (ICTV) (Barylski et al., 2020; Turner et al., 2021).

During genomes analyses of phages Ristretto and Corretto, no genes associated with integration, recombination, virulence, or antibiotic resistance were found, further supporting their potential for therapeutic use in treating infections caused by *C. acnes*. The absence of these genes is crucial as it minimizes the risk of horizontal gene transfer, adverse host interactions, and the unintended spread of antibiotic resistance, ensuring the safety and efficacy of phage-based therapies. Similarly, reports of some other *C. acnes* phages also show therapeutic potential by lacking these genes. For example phage Y3Z showed no virulence-related genes, antibiotic resistance genes or tRNA (Xuan et al., 2023). Phage P105, the closest relative of phage Ristretto, and phage P100D which exhibited the greatest similarity to phage Corretto, both lacked genes encoding integrase (Marinelli et al., 2012).

Newly isolated phages Ristretto and Corretto show high therapeutic potential against clinical *C. acnes* strains and anti-biofilm properties. However, one important limitation of this study is that only seven out of 21 tested *C. acnes* strains were identified to form strong biofilm. Among these, only three were susceptible to infection by phage Ristretto, limiting our ability to assess its broader anti-biofilm efficacy. Further research could address this limitation by incorporating a larger collection of biofilm-forming *C. acnes* strains and expanding the analysis to include transcriptomic and proteomic studies to better understand the phage's anti-biofilm mechanisms.

## 5. Conclusion

Both, phage Ristretto and Corretto are genetically distinct bacteriophages that display specific antibacterial effect, setting them apart as promising candidates for therapeutic use. In terms of their characteristics, they fulfil all the criteria required for bacteriophages to be suitable for treatment. Future research should explore the anti-biofilm effects of our bacteriophages in the form of a phage cocktail and assess their impact on biofilms developed on orthopaedic and dental materials commonly used in prostheses.

We believe that the use of these bacteriophages holds significant potential in addressing *C. acnes*-induced pathologies. These include not only acne but also infections associated with orthopaedic prostheses and dental implants. Furthermore, their ability to disrupt biofilms suggests they could be particularly effective in managing peri-implantitis, presenting a promising strategy for advancing dermatological, orthopaedic and dental health treatments.

## CRedit authorship contribution statement

**Anja Frantar:** Writing – original draft, Visualization, Investigation, Formal analysis, Data curation, Conceptualization. **Rok Gašperšič:** Writing – review & editing, Supervision, Resources. **Katja Seme:** Writing – review & editing, Supervision, Resources. **Katja Šuster:** Writing – review & editing, Writing – original draft, Visualization, Supervision, Software, Resources, Methodology, Investigation, Formal analysis, Data curation, Conceptualization. **Cedomir Oblak:** Writing – review & editing, Supervision, Resources.

## Ethics approval

The study was approved by the Medical Ethics Committee of Valdoltra Orthopaedic Hospital (Ethics number: 07/2023, 30 June 2023) and by the National Medical Ethics Committee of the Republic of Slovenia (Ethics number: 0120-535/2023/3, 19 January 2024).

## Funding

This research was funded by the Slovenian Research and Innovation Agency (grant numbers Z3-4506 and P3-0374).

## Declaration of Competing Interest

The authors declare no competing interests.

## Appendix A. Supporting information

Supplementary data associated with this article can be found in the online version at [doi:10.1016/j.ijmm.2025.151668](https://doi.org/10.1016/j.ijmm.2025.151668).

## Data availability

Data will be made available on request.

## References

- Ahmed, S.S., Haddad, F.S., 2019. Prosthetic joint infection. *Bone Jt. Res.* 8, 570–572.
- Almouhrabie, S., Cau, L., Cavagnero, K., O'Neill, A.M., Li, F., Roso-Mares, A., Mainzer, C., Closs, B., Kolar, M.J., Williams, K.J., Bensinger, S.J., Gallo, R.L., 2023. Commensal cutibacterium acnes induce epidermal lipid synthesis important for skin barrier function. *Sci. Adv.* 9, eadg6262.
- Alp, E., Cevahir, F., Ersoy, S., Guney, A., 2016. Incidence and economic burden of prosthetic joint infections in a university hospital: a report from a middle-income country. *J. Infect. Public Health* 9, 494–498.
- Altschul, S.F., Madden, T.L., Schäffer, A.A., Zhang, J., Zhang, Z., Miller, W., Lipman, D.J., 1997. Gapped BLAST and PSI-BLAST: a new generation of protein database search programs. *Nucleic Acids Res.* 25, 3389–3402.
- Arciola, C.R., Campoccia, D., Montanaro, L., 2018. Implant infections: adhesion, biofilm formation and immune evasion. *Nat. Rev. Microbiol.* 16, 397–409.
- Aslam, S., Lampley, E., Wooten, D., Karris, M., Benson, C., Strathdee, S., Schooley, R.T., 2020. Lessons learned from the first 10 consecutive cases of intravenous bacteriophage therapy to treat multidrug-resistant bacterial infections at a single center in the United States. *Open Forum Infect. Dis.* 7.
- Association, W.M., 2025. World medical association declaration of Helsinki: ethical principles for medical research involving human participants. *JAMA* 333, 71–74.
- Bai, X., Shen, Y., Zhang, T., Meng, R., Zhang, Y., Deng, Y., Guo, N., 2023. Anti-biofilm activity of biochanin A against *Staphylococcus aureus*. *Appl. Microbiol. Biotechnol.* 107, 867–879.
- Barylski, J., Kropinski, A.M., Alikhan, N.-F., Adriaenssens, E.M., Consortium, I.R., 2020. ICTV virus taxonomy profile: herelleviridae. *J. Gen. Virol.* 101, 362–363.
- Bayston, R., Ashraf, W., Barker-Davies, R., Tucker, E., Clement, R., Clayton, J., Freeman, B.J.C., Nuradeen, B., 2007. Biofilm formation by propionibacterium acnes on biomaterials in vitro and in vivo: impact on diagnosis and treatment. *J. Biomed. Mater. Res. Part A* 81A, 705–709.
- Blomstrom-Lundqvist, C., Ostrowska, B., 2021. Prevention of cardiac implantable electronic device infections: guidelines and conventional prophylaxis. *EP Eur.* 23, iv11–iv19.
- Boisrenoult, P., 2018. Cutibacterium acnes prosthetic joint infection: diagnosis and treatment. *Orthop. Traumatol. Surg. Res.* OTSR 104, S19–S24.
- Bonilla, N., Rojas, M.I., Netto Flores Cruz, G., Hung, S.H., Rohwer, F., Barr, J.J., 2016. Phage on tap—a quick and efficient protocol for the preparation of bacteriophage laboratory stocks. *PeerJ* 4, e2261.
- Bortolaia, V., Kaas, R.S., Ruppe, E., Roberts, M.C., Schwarz, S., Cattoir, V., Philippon, A., Allesoe, R.L., Rebelo, A.R., Florensa, A.F., Fagelhauer, L., Chakraborty, T., Neumann, B., Werner, G., Bender, J.K., Stingsl, K., Nguyen, M., Coppins, J., Xavier, B. B., Malhotra-Kumar, S., Westh, H., Pinholt, M., Anjum, M.F., Duggett, N.A., Kempf, I., Nykäsenoja, S., Olkkola, S., Wiczorek, K., Amaro, A., Clemente, L., Mossong, J., Losch, S., Ragimbeau, C., Lund, O., Aarestrup, F.M., 2020. ResFinder 4.0 for predictions of phenotypes from genotypes. *J. Antimicrob. Chemother.* 75, 3491–3500.
- Bossard, D.A., Ledergerber, B., Zingg, P.O., Gerber, C., Zinkernagel, A.S., Zbinden, R., Achermann, Y., 2016. Optimal length of cultivation time for isolation of propionibacterium acnes in suspected bone and joint infections is more than 7 days. *J. Clin. Microbiol.* 54, 3043–3049.
- Brown, T.L., Petrovski, S., Dyson, Z.A., Seviour, R., Tucci, J., 2016. The formulation of bacteriophage in a semi solid preparation for control of propionibacterium acnes growth. *PLOS ONE* 11, e0151184.
- Camacho, C., Coulouris, G., Avagyan, V., Ma, N., Papadopoulos, J., Bealer, K., Madden, T.L., 2009. BLAST+: architecture and applications. *BMC Bioinforma.* 10, 421.
- Chen, B., Chittò, M., Tao, S., Wagemans, J., Lavigne, R., Richards, R.G., Metsemakers, W.-J., Moriarty, T.F., 2024. Isolation and antibiofilm activity of bacteriophages against cutibacterium acnes from patients with periprosthetic joint infection. *Viruses* 16, 1592.
- Cheng, L., Marinelli, L.J., Grosset, N., Fitz-Gibbon, S.T., Bowman, C.A., Dang, B.Q., Russell, D.A., Jacobs-Sera, D., Shi, B., Pellegrini, M., Miller, J.F., Gautier, M., Hatfull, G.F., Modlin, R.L., 2018. Complete genomic sequences of Propionibacterium freudenreichii phages from Swiss cheese reveal greater diversity than cutibacterium (formerly Propionibacterium) acnes phages. *BMC Microbiol.* 18, 19.
- Chopin, M.C., Rouault, A., Ehrlich, S.D., Gautier, M., 2002. Filamentous phage active on the gram-positive bacterium propionibacterium freudenreichii. *J. Bacteriol.* 184, 2030–2033.
- Coenye, T., Spittaels, K.J., Achermann, Y., 2022. The role of biofilm formation in the pathogenesis and antimicrobial susceptibility of cutibacterium acnes. *Biofilm* 4, 100063.
- Cros, M.P., Mir-Pedrol, J., Toloza, L., Knödseder, N., Maruotti, J., Zouboulis, C.C., Güell, M., Fábrega, M.-J., 2023. New insights into the role of cutibacterium acnes-derived extracellular vesicles in inflammatory skin disorders. *Sci. Rep.* 13, 16058.
- Das, T., Sehar, S., Koop, L., Wong, Y.K., Ahmed, S., Siddiqui, K.S., Manefield, M., 2014. Influence of calcium in extracellular DNA mediated bacterial aggregation and biofilm formation. *PLOS ONE* 9, e91935.
- Dioguardi, M., Alovisi, M., Crincoli, V., Aiuto, R., Malagnino, G., Quarta, C., Laneve, E., Sovereto, D., Lo Russo, L., Troiano, G., Lo Muzio, L., 2020. Prevalence of the genus propionibacterium in primary and persistent endodontic lesions: a systematic review. *J. Clin. Med.* 9, 739.
- Domingo-Calap, P., Delgado-Martínez, J., 2018. Bacteriophages: protagonists of a post-antibiotic era. *Antibiotics* 7, 66.
- Dréno, B., Pécastings, S., Corvec, S., Veraldi, S., Khammari, A., Roques, C., 2018. Cutibacterium acnes (Propionibacterium acnes) and acne vulgaris: a brief look at the latest updates. *J. Eur. Acad. Dermatol. Venereol. JEADV* 32 (2), 5–14.
- Egido, J.E., Costa, A.R., Aparicio-Maldonado, C., Haas, P.J., Brouns, S.J.J., 2022. Mechanisms and clinical importance of bacteriophage resistance. *FEMS Microbiol. Rev.* 46.
- Emery, D.C., Shoemark, D.K., Batstone, T.E., Waterfall, C.M., Coghill, J.A., Cerajewska, T.L., Davies, M., West, N.X., Allen, S.J., 2017. 16S rRNA next generation sequencing analysis shows bacteria in Alzheimer's post-mortem brain. *Front. Aging Neurosci.* 9.
- Exarchos, V., Tkhalishvili, T., Potapov, E., Starck, C., Trampuz, A., Schoenrath, F., 2020. Successful bacteriophage treatment of infection involving cardiac implantable electronic device and aortic graft: a trojan horse concept. *EP Europace* 22, 597–597.
- Fowler, B.J., Miller, D., Yan, X., Yannuzzi, N.A., Flynn Jr., H.W., 2021. Postoperative endophthalmitis caused by cutibacterium (Formerly Propionibacterium) acnes: case series and review. *Case Rep. Ophthalmol.* 12, 1–10.
- García, D., Mayfield, C.K., Leong, J., Deckey, D.G., Zega, A., Glasser, J., Daniels, A.H., Ebersson, C., Green, A., Born, C., 2020. Early adherence and biofilm formation of cutibacterium acnes (formerly Propionibacterium acnes) on spinal implant materials. *Spine J. Off. J. North Am. Spine Soc.* 20, 981–987.
- Garneau, J.R., Depardieu, F., Fortier, L.C., Bikard, D., Monot, M., 2017. PhageTerm: a tool for fast and accurate determination of phage termini and packaging mechanism using next-generation sequencing data. *Sci. Rep.* 7, 8292.
- Geng, Y., Nguyen, T.V.P., Homaee, E., Golding, I., 2024. Using bacterial population dynamics to count phages and their lysogens. *Nat. Commun.* 15, 7814.
- Golembo, M., Puttagunta, S., Rappo, U., Weinstock, E., Engelstein, R., Gahali-Sass, I., Moses, A., Kario, E., Ben-Dor Cohen, E., Nicenboim, J., Ben David, H., Sudakov, K., Cohen, A., Bassan, M., Zak, N.B., 2022. Development of a topical bacteriophage gel targeting cutibacterium acnes for acne prone skin and results of a phase I cosmetic randomized clinical trial. *Ski. Health Dis.* 2, e93.
- Gurevich, A., Saveliev, V., Vyahhi, N., Tesler, G., 2013. QUAST: quality assessment tool for genome assemblies. *Bioinformatics (Oxford, England)* 29, 1072–1075.
- Han, M.-H., Khan, S.A., Moon, G.-S., 2023. Cutibacterium acnes KCTC 3314 growth reduction with the combined use of bacteriophage PAP 1-1 and nisin. *Antibiotics*.
- Herrera, D., Berglund, T., Schwarz, F., Chapple, I., Jepsen, S., Sculean, A., Kerschull, M., Papapanou, P.N., Tonetti, M.S., Sanz, M., participants, tEw, consultant, m, 2023. Prevention and treatment of peri-implant diseases—The EFP S3 level clinical practice guideline. *J. Clin. Periodontol.* 50, 4–76.
- Høyland-Kroghsbo, N.M., Maerkedahl, R.B., Svenningsen, S.L., 2013. A quorum-sensing-induced bacteriophage defense mechanism. *mBio* 4, e00362–00312.
- Hyman, P., 2019. Phages for phage therapy: isolation, characterization, and host range breadth. *Pharmaceuticals* 12, 35.
- Kennedy, D.G., O'Mahony, A.M., Culligan, E.P., O'Driscoll, C.M., Ryan, K.B., 2022. Strategies to mitigate and treat orthopaedic device-associated infections. *Antibiotics* 11, 1822.
- Kim, M.K., Chen, Q., Echterhof, A., Pennetzdorfer, N., McBride, R.C., Banaei, N., Burgener, E.B., Milla, C.E., Bollyky, P.L., 2024. A blueprint for broadly effective bacteriophage-antibiotic cocktails against bacterial infections. *Nat. Commun.* 15, 9987.
- Kim, S., Song, H., Jin, J.S., Lee, W.J., Kim, J., 2022. Genomic and phenotypic characterization of cutibacterium acnes bacteriophages isolated from acne patients. *Antibiotics* 11, 1041.
- Kolenbrander, P.E., Palmer, R.J., Periasamy, S., Jakubovics, N.S., 2010. Oral multispecies biofilm development and the key role of cell–cell distance. *Nat. Rev. Microbiol.* 8, 471–480.
- Kröger, A., Hülsmann, C., Fickl, S., Spinell, T., Hüttig, F., Kaufmann, F., Heimbach, A., Hoffmann, P., Enkling, N., Renvert, S., Schwarz, F., Demmer, R.T., Papapanou, P.N., Jepsen, S., Kerschull, M., 2018. The severity of human peri-implantitis lesions correlates with the level of submucosal microbial dysbiosis. *J. Clin. Periodontol.* 45, 1498–1509.
- Kropinski, A.M., Mazzocco, A., Waddell, T.E., Lingohr, E., Johnson, R.P., 2009. Enumeration of bacteriophages by double agar overlay plaque assay. In: Clokie, M.R. J., Kropinski, A.M. (Eds.), *Bacteriophages: Methods and Protocols*, Volume 1: Isolation, Characterization, and Interactions. Humana Press, Totowa, NJ, pp. 69–76.
- Kutter, E., Sulakvelidze, A., 2004. Bacteriophages: biology and applications. CRC Press.
- Lam, H.Y.P., Lai, M.-J., Chen, T.-Y., Wu, W.-J., Peng, S.-Y., Chang, K.-C., 2021. Therapeutic effect of a newly isolated lytic bacteriophage against multi-drug-resistant Cutibacterium acnes infection in mice. *Int. J. Mol. Sci.* 22, 7031.
- Li, X., Ding, W., Li, Z., Yan, Y., Tong, Y., Xu, J., Li, M., 2024. vB\_CacS-HV1 as a novel pahexavirus bacteriophage with lytic and anti-biofilm potential against cutibacterium acnes. *Microorganisms* 12, 1566.

- Liao, D., Zhang, J., Liu, R., Chen, K., Liu, Y., Shao, Y., Shi, X., Zhang, Y., Yang, Z., 2023. Whole-genome sequencing, annotation, and biological characterization of a novel siphoviridae phage against multi-drug resistant *Propionibacterium* acne. *Front. Microbiol.* 13.
- Little, J.S., Dedrick, R.M., Freeman, K.G., Cristinziano, M., Smith, B.E., Benson, C.A., Jhaveri, T.A., Baden, L.R., Solomon, D.A., Hatfull, G.F., 2022. Bacteriophage treatment of disseminated cutaneous *Mycobacterium chelonae* infection. *Nat. Commun.* 13, 2313.
- Liu, J., Yan, R., Zhong, Q., Ngo, S., Bangayan, N.J., Nguyen, L., Lui, T., Liu, M., Erfe, M. C., Craft, N., Tomida, S., Li, H., 2015. The diversity and host interactions of propionibacterium acnes bacteriophages on human skin. *ISME J.* 9, 2078–2093.
- Liu, Y., Zhen, N., Liao, D., Niu, J., Liu, R., Li, Z., Lei, Z., Yang, Z., 2024. Application of bacteriophage  $\phi$ PaP11-13 attenuates rat cutibacterium acnes infection lesions by promoting keratinocytes apoptosis via inhibiting PI3K/Akt pathway. *Microbiol. Spectr.* 12, e0283823.
- Marinelli, L.J., Fitz-Gibbon, S., Hayes, C., Bowman, C., Inkeles, M., Loncaric, A., Russell, D.A., Jacobs-Sera, D., Cokus, S., Pellegrini, M., Kim, J., Miller, J.F., Hatfull, G.F., Modlin, R.L., 2012. *Propionibacterium acnes* bacteriophages display limited genetic diversity and broad killing activity against bacterial skin isolates. *mBio* 3.
- Mayslich, C., Grange, P.A., Dupin, N., 2021. Cutibacterium acnes as an opportunistic pathogen: an update of its virulence-associated factors. *Microorganisms* 9.
- McNair, K., Zhou, C., Dinsdale, E.A., Souza, B., Edwards, R.A., 2019. PHANOTATE: a novel approach to gene identification in phage genomes. *Bioinformatics (Oxford, England)* 35, 4537–4542.
- Monje, A., Insua, A., Wang, H.L., 2019. Understanding Peri-Implantitis as a plaque-associated and site-specific entity: on the local predisposing factors. *J. Clin. Med.* 8.
- Moraru, C., Varsani, A., Kropinski, A.M., 2020. VIRIDIC-a novel tool to calculate the intergenomic similarities of Prokaryote-Infecting viruses. *Viruses* 12.
- Ngiam, L., Weynberg, K., Guo, J., 2024. Evolutionary and co-evolutionary phage training approaches enhance bacterial suppression and delay the emergence of phage resistance. *ISME Commun.* 4, ycae082.
- Niazi, S.A., Al Kharusi, H.S., Patel, S., Bruce, K., Beighton, D., Foschi, F., Mannocci, F., 2016. Isolation of propionibacterium acnes among the microbiota of primary endodontic infections with and without intraoral communication. *Clin. Oral. Investig.* 20, 2149–2160.
- Nishimura, Y., Yamada, K., Okazaki, Y., Ogata, H., 2024. DiGAlign: versatile and interactive visualization of sequence alignment for comparative genomics. *Microbes Environ.* 39.
- Nishimura, Y., Yoshida, T., Kuronishi, M., Uehara, H., Ogata, H., Goto, S., 2017. ViPTree: the viral proteomic tree server. *Bioinformatics (Oxford, England)* 33, 2379–2380.
- Noguchi, H., Taniguchi, T., Itoh, T., 2008. MetaGeneAnnotator: detecting species-specific patterns of ribosomal binding site for precise gene prediction in anonymous prokaryotic and phage genomes. *DNA Res. Int. J. Rapid Publ. Rep. Genes Genomes* 15, 387–396.
- Ooi, M.L., Drilling, A.J., Morales, S., Fong, S., Moraitis, S., Macias-Valle, L., Vreugde, S., Psaltis, A.J., Wormald, P.-J., 2019. Safety and tolerability of bacteriophage therapy for chronic rhinosinusitis due to staphylococcus aureus. *JAMA Otolaryngol. Head. Neck Surg.* 145, 723–729.
- Otto-Lambertz, C., Yagdiran, A., Wallscheid, F., Eysel, P., Jung, N., 2017. Periprosthetic infection in joint replacement. *Dtsch. Arzteblatt Int.* 114, 347–353.
- Park, J.Y., Han, D., Park, Y., Cho, E.S., In Yook, J., Lee, J.S., 2024. Intracellular infection of Cutibacterium acnes in macrophages of extensive peri-implantitis lesions: A clinical case series. *Clin Implant Dent Relat Res* 26, 1126–1134.
- Patel, P.M., Camps, N.S., Rivera, C.I., Gomez, I., Tuda, C.D., 2022. Cutibacterium acnes: an emerging pathogen in culture negative bacterial prosthetic valve infective endocarditis (IE). *IDCases* 29, e01555.
- Pires, D.P., Melo, L.D.R., Azeredo, J., 2021. Understanding the complex phage-host interactions in biofilm communities. *Annu. Rev. Virol.* 8, 73–94.
- Pires, D.P., Oliveira, H., Melo, L.D.R., Sillankorva, S., Azeredo, J., 2016. Bacteriophage-encoded depolymerases: their diversity and biotechnological applications. *Appl. Microbiol. Biotechnol.* 100, 2141–2151.
- Radaic, A., Kapila, Y.L., 2021. The oralome and its dysbiosis: new insights into oral microbiome-host interactions. *Comput. Struct. Biotechnol. J.* 19, 1335–1360.
- Rakic, M., Galindo-Moreno, P., Monje, A., Radovanovic, S., Wang, H.L., Cochran, D., Sculean, A., Canullo, L., 2018. How frequent does peri-implantitis occur? A systematic review and meta-analysis. *Clin. Oral. Investig.* 22, 1805–1816.
- Rimon, A., Rakov, C., Lerer, V., Sheffer-Levi, S., Oren, S.A., Shlomov, T., Shasha, L., Lubin, R., Zubeidat, K., Jaber, N., Mujahed, M., Wilensky, A., Copenhagen-Glazer, S., Molho-Pessach, V., Hazan, R., 2023. Topical phage therapy in a mouse model of cutibacterium acnes-induced acne-like lesions. *Nat. Commun.* 14, 1005.
- Sayers, E.W., Agarwala, R., Bolton, E.E., Brister, J.R., Canese, K., Clark, K., Connor, R., Fiorini, N., Funk, K., Hefferon, T., Holmes, J.B., Kim, S., Kimchi, A., Kitts, P.A., Lathrop, S., Lu, Z., Madden, T.L., Marchler-Bauer, A., Phan, L., Schneider, V.A., Schoch, C.L., Pruitt, K.D., Ostell, J., 2019. Database resources of The National Center for Biotechnology Information. *Nucleic Acids Res.* 47, D23–d28.
- Seemann, T., 2014. Prokka: rapid prokaryotic genome annotation. *Bioinformatics (Oxford, England)* 30, 2068–2069.
- Simmons, E.L., Bond, M.C., Koskella, B., Drescher, K., Bucci, V., Nadell, C.D., 2020. Biofilm structure promotes coexistence of phage-resistant and phage-susceptible bacteria. *mSystems* 5.
- Talank, N., Morad, H., Barabadi, H., Mojab, F., Amidi, S., Kobarfard, F., Mahjoub, M.A., Jounaki, K., Mohammadi, N., Salehi, G., Ashrafzadeh, M., Mostafavi, E., 2022. Bioengineering of Green-synthesized silver nanoparticles: in vitro physicochemical, antibacterial, biofilm inhibitory, anticoagulant, and antioxidant performance. *Talanta* 243, 123374.
- Tkhilaishvili, T., Winkler, T., Müller, M., Perka, C., Trampuz, A., 2019. Bacteriophages as adjuvant to antibiotics for the treatment of periprosthetic joint infection caused by multidrug-resistant *Pseudomonas aeruginosa*. *Antimicrob. Agents Chemother.* 64.
- Turner, D., Kropinski, A.M., Adriaenssens, E.M., 2021. A roadmap for genome-based phage taxonomy. *Viruses* 13, 506.
- Ugge, H., Carlsson, J., Söderquist, B., Fall, K., Andén, O., Davidsson, S., 2018. The influence of prostatic cutibacterium acnes infection on serum levels of IL6 and CXCL8 in prostate cancer patients. *Infect. Agents Cancer* 13, 34.
- Wang, P., Jiao, Y., Liu, S., 2014. Novel fermentation process strengthening strategy for production of propionic acid and vitamin B12 by propionibacterium freudenreichii. *J. Ind. Microbiol. Biotechnol.* 41, 1811–1815.
- Weber-Dąbrowska, B., Mulczyk, M., Górski, A., 2003. Bacteriophages as an efficient therapy for antibiotic-resistant septicemia in man. *Transplant. Proc.* 35, 1385–1386.
- Weinstein, R.A., Darouiche, R.O., 2001. Device-associated infections: a macroproblem that starts with microadherence. *Clin. Infect. Dis.* 33, 1567–1572.
- Wick, R.R., Judd, L.M., Gorrie, C.L., Holt, K.E., 2017. Unicycler: resolving bacterial genome assemblies from short and long sequencing reads. *PLoS Comput. Biol.* 13, e1005595.
- Winans, J.B., Wucher, B.R., Nadell, C.D., 2022. Multispecies biofilm architecture determines bacterial exposure to phages. *PLOS Biol.* 20, e3001913.
- Wu, N., Dai, J., Guo, M., Li, J., Zhou, X., Li, F., Gao, Y., Qu, H., Lu, H., Jin, J., Li, T., Shi, L., Wu, Q., Tan, R., Zhu, M., Yang, L., Ling, Y., Xing, S., Zhang, J., Yao, B., Le, S., Gu, J., Qin, J., Li, J., Cheng, M., Tan, D., Li, L., Zhang, Y., Zhu, Z., Cai, J., Song, Z., Guo, X., Chen, L.-K., Zhu, T., 2021. Pre-optimized phage therapy on secondary acinetobacter baumannii infection in four critical COVID-19 patients. *Emerg. Microbes Infect.* 10, 612–618.
- Xuan, G., Wang, Y., Wang, Y., Lin, H., Wang, C., Wang, J., 2023. Characterization of the newly isolated phage Y3Z against multi-drug resistant cutibacterium acnes. *Microb. Pathog.* 180, 106111.